STUDY OF MICROSTRUCTURAL CHARACTERISTICS USING MATHEMATICAL MORPHOLOGY

Mathew S. Chackalackal and John P. Basart
Department of Electrical and Computer Engineering
Center for Nondestructive Evaluation
Iowa State University
Ames, Iowa 50011

INTRODUCTION

In NDE images, one often comes across overlapping or connected regions of interest. Segmentation of these regions becomes one of the preprocessing stages before any kind of image analysis. A secondary electron image showing silicon carbide particles dispersed in aluminum metal matrix composites is given in Figure 1. To study the microstructural characteristics of these composites, segmentation of the various particles is essential. Segmentation of these particles using conditional skeleton was about forty percent successful [1]. Three different approaches with varying degrees of complexity and accuracy are discussed in this paper. All three techniques are based on the principles of mathematical morphology [2]. The first step in all three techniques is to generate a marker or seed for each particle in the image. Once the seeds are generated, the techniques differ in the manner in which the seeds are grown. All the techniques work on binary images. Experimental results with microstructural statistics for each technique are presented in the paper. Some of the advanced morphological tools used are defined in the next section

Figure 1. Secondary electron image of a metal matrix composite.

Review of Progress in Quantitative Nondestructive Evaluation, Vol. 11
Edited by D.O. Thompson and D.E. Chimenti, Plenum Press, New York, 1992

DEFINITIONS

Conditional Dilation: The conditional dilation of $\mathbf{A}$ by $\mathbf{B}$ with respect to $\mathbf{X}$ is denoted by $\mathbf{A} \oplus \mathbf{B}; \mathbf{X}$ and is defined by [3]:

$$\mathbf{A} \oplus \mathbf{B}; \mathbf{X} = (\mathbf{A} \oplus \mathbf{B}) \cap \mathbf{X}. \tag{1}$$

where $\oplus$ indicates dilation. Here the conditionally dilated image contains the elements common to the image $\mathbf{X}$ and the result of $\mathbf{A}$ dilated by $\mathbf{B}$.

Sequential Conditional Dilation: The sequential conditional dilation of $\mathbf{A}$ by $\mathbf{B}$ is denoted by $\mathbf{A} \oplus \{\mathbf{B}\}; \mathbf{X}$ and is defined by:

$$\mathbf{A} \oplus \{\mathbf{B}\}; \mathbf{X} = \cdots [[[(\mathbf{A} \oplus \mathbf{B}) \cap \mathbf{X}] \oplus \mathbf{B}] \cap \mathbf{X}] \oplus \mathbf{B} \cdots. \tag{2}$$

Here $\mathbf{A}$ is repeatedly conditionally dilated by $\mathbf{B}$ until the resulting image ceases to grow. As in the case of conditional dilation $\mathbf{X}$ is the limiting image. This is a very important tool in connectivity analysis as it can be used to retrieve particles that were lost during the erosion process.

Thickening: The thickening of $\mathbf{X}$ by $\mathbf{T}$ is denoted by $\mathbf{X} \odot \mathbf{T}$. Thickening is different from dilation. It differs mainly in the nature of the structuring element. The structuring element does not contain the origin and it checks both the image and its background. Figure 2 illustrates thickening. $\mathbf{A}$ is the image and $\mathbf{T}$ is the structuring element. A one is placed at the origin if the zeros in the structuring element hits the background and the ones of the structuring element hit the image. $\mathbf{C}$ is the thickened image.

Sequential Conditional Thickening: The sequential conditional thickening of $\mathbf{Y}$ by $\mathbf{T}$ with respect to the limiting set $\mathbf{X}$ is given by $\mathbf{Y} \odot \{\mathbf{T}^i\}; \mathbf{X}$ and is similar to sequential conditional dilation. $\mathbf{T}^i$ denotes a series of 'i' structuring elements.

METHOD 1

Figure 3 shows particles that are roughly the same size and barely touching. An erosion by a unit disk will break the connectivity among the various particles. Method 1 is an extension of this technique. It involves erosion by a large disk to break the connectivity among the various particles. An image expansion is performed before regrowing the eroded particles to prevent the particles from reconnecting.

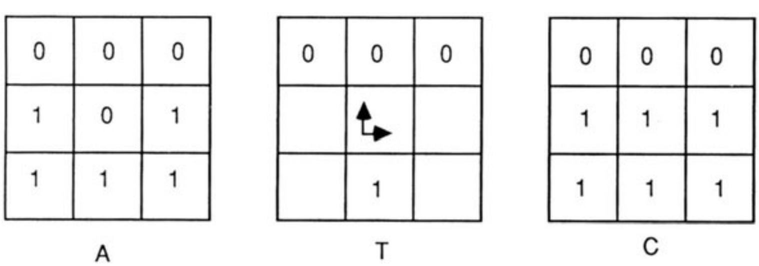

Figure 2. Illustration of thickening.

Step 1:

$$\mathbf{Y} = \mathbf{X} \ominus m\mathbf{B} \tag{3}$$

where $\mathbf{X}$ is the original image, $\mathbf{Y}$ is the eroded image, and $\mathbf{B}$ is a disk of unit radius. The image is eroded by a disk of radius m such that the connectivity among most of the particles is broken. The radius of the structuring element is decided by visual inspection. Hence this technique is not fully automated.

Step 2:
Particles smaller than $m\mathbf{B}$ disappear as a result of the erosion. The particles that disappear are retrieved using sequential conditional dilation. $\mathbf{Z}$ contains the retrieved particles and is given by

$$\mathbf{Z} = \mathbf{X} - (\mathbf{Y} \oplus \{\mathbf{B}\};\mathbf{X}). \tag{4}$$

The connectivity among retrieved particles cannot be broken using this technique.

Step 3:
Particles in $\mathbf{Y}$ and $\mathbf{Z}$ are labelled using principles of eight connectivity. Pixels belonging to an isolated particle are given a unique integer label. The centroids for each labelled particle in $\mathbf{Y}$ and $\mathbf{Z}$ are determined. $\mathbf{Y}$ and $\mathbf{Z}$ are treated as two different images.

Step 4:
Image expansions are performed on $\mathbf{Y}$ and $\mathbf{Z}$. An n x n image becomes 2n x 2n. The centroids of the various particles determined in *Step 3* are used as reference points in the transformation. A centroid at location (k, l) gets transformed to (2k, 2l) on the expanded image. The remaining pixels for each particle are transformed with respect to the corresponding centroid. This keeps the size and the orientation of the particles unchanged. $\mathbf{Y}$ and $\mathbf{Z}$ have been transformed to $\bar{\mathbf{Y}}$ and $\bar{\mathbf{Z}}$.

Step 5:
The eroded and expanded image, $\bar{\mathbf{Y}}$, is regrown by dilation with a disk of radius $m\mathbf{B}$. The original image was eroded by a disk of radius $m\mathbf{B}$. Image expansion in Step 4 prevents the particles from reconnecting. The resulting image is given by

$$\mathbf{V} = \bar{\mathbf{Y}} \oplus m\mathbf{B}. \tag{5}$$

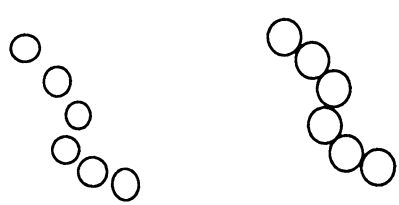

Figure 3. Simple connectivity analysis.

Step 6:
The dilated image is then combined with the transformed residual image to obtain the final image given by

$$\mathbf{U} = \mathbf{V} \cup \bar{\mathbf{Z}}. \tag{6}$$

Figure 4a is a subimage of the image in Figure 1. The image in Figure 4a is eroded by a disk of radius fifteen. The radius of the disk was chosen by visual inspection and as can be seen, the connectivity among the various particles have been broken. The particles in Figure 4a that were smaller than the eroding disk are not present in the eroded image. The result of Method 1 is given in Figure 4b. As can be seen, the connectivity among the various particles have been broken. But this technique fails to faithfully reproduce the original particles.

CLUSTER FAST SEGMENTATION

The next two techniques depend on cluster fast segmentation to find markers or seeds for every particle in the image. Cluster fast segmentation (CFS) is a morphological algorithm that breaks the connectivity among convex flaws that appear in a cluster. The underlying principle is to find a marker for every individual particle that exists in the cluster. Once the markers are obtained, the three techniques differ in the manner in which they are grown back. The steps involved in CFS are as listed. $\mathbf{X}$ is the image and $\mathbf{B}$ is a unit circle.

Step 1:

$$\mathbf{X}_i = \mathbf{X} \ominus iB, for \ \ i = 1, \cdot\cdot, m \ \ where \ \{m : \mathbf{X}_m \neq \emptyset\}. \tag{7}$$

$\mathbf{X}_1 = \mathbf{X} \ominus B$, $\mathbf{X}_2 = \mathbf{X} \ominus 2B$, and so on until $\mathbf{X}_m = \mathbf{X} \ominus mB$, and $\mathbf{X}_{m+1} = \emptyset$. Here the image is repeatedly eroded by a unit circle until it ceases to exist. All the subsequent stages in the erosion process are saved. The objective here is to break the connectivity among the various particles. Since we repeatedly erode till the image ceases to exist, the connectivity among the various particles would have been broken somewhere down the line.

Step 2 (Ultimate Erosion):

$$\mathbf{Y}_i = \mathbf{X}_i / (\mathbf{X}_{i+1} \oplus \{B\}; \mathbf{X}_i). \tag{8}$$

Figure 4. Result of applying Method 1.

Here the $\mathbf{Y}_i$s are the ultimate eroded sets or the seeds. Each $\mathbf{Y}_i$ consists of the ultimate eroded sets of particles that existed in $\mathbf{X}_i$, but not in $\mathbf{X}_{i+1}$. An ultimate eroded set of a particle is that stage, during repeated erosions, after which the particle ceases to exist. There will be as many seeds as there are particles. The seed generated for each particle will serve as the marker for that particle in the algorithm.

METHOD 2

As mentioned earlier, this technique incorporates the principles of cluster fast segmentation and image expansion used in Method 1. This technique is fully automated.

This technique does not faithfully reproduce the original shape and size of the particles. But as mentioned earlier, this technique is fully automated. The major drawback of Method 1 is its incapability to faithfully reproduce the size and shape of the parent particles. Since the objective is to determine the orientation of the particles, it is important to approximate the original particles as closely as possible. The limitation of Method 1 is due to the nature of the disk, which is shaped like a cross for the size of our structuring element. To overcome this limitation, structuring elements in four different orientations were used during the regrowing process. The difference this brings about is remarkable.

Step 1:
This is similar to Step 1 of CFS.

Step 2 (Ultimate Erosion):
This is identical to Step 2 of CFS.

Step 3:
$\mathbf{B}_1, \mathbf{B}_2, \mathbf{B}_3$, and $\mathbf{B}_4$ are structuring elements in the four different orientations discussed above. $\mathbf{U}_1, \mathbf{U}_2, \mathbf{U}_3$, and $\mathbf{U}_4$ are the results of dilating the ultimate eroded sets by $\mathbf{B}_1, \mathbf{B}_2, \mathbf{B}_3$, and $\mathbf{B}_4$ respectively, and $\mathbf{U}_i$ is obtained by taking the union of the four results. Thus,

$$\mathbf{U}_{i1} = \mathbf{Y}_i \oplus (m+2)\mathbf{B}_1 \tag{9}$$
$$\mathbf{U}_{i2} = \mathbf{Y}_i \oplus (m+2)\mathbf{B}_2 \tag{10}$$
$$\mathbf{U}_{i3} = \mathbf{Y}_i \oplus (m+2)\mathbf{B}_3 \tag{11}$$
$$\mathbf{U}_{i4} = \mathbf{Y}_i \oplus (m+2)\mathbf{B}_4 \tag{12}$$
$$\mathbf{U}_i = \mathbf{U}_{i1} \cup \mathbf{U}_{i2} \cup \mathbf{U}_{i3} \cup \mathbf{U}_{i4} \tag{13}$$

Step 4:
A set intersection between the dilated ultimate eroded set and the original image is performed to reproduce the original particle shape as faithfully as possible. This is given by

$$\mathbf{V}_i = \mathbf{U}_i \cap \mathbf{X}. \tag{14}$$

Step 5:
Step 3 of Method 1 is performed on $\mathbf{V}_i$. Using the centroids as reference, the particles in $\mathbf{V}_i$ are transformed onto $\mathbf{Z}$ which has twice the dimensions of $\mathbf{X}$. Steps 3, 4, and 5 are repeated for $i = 1, \cdots, m$.

Figure 5a is the original image and Figure 5b is the result of Method 2. This technique had done a fairly good job in breaking the connectivity among the various particles and faithfully reproducing the original particles. It is fully automated and more time consuming than Method 1.

SEGMENTATION BY WATERSHEDS

The two methods discussed so far require an image expansion before regrowing the seeds. This could impose a constraint on the size of the original image that could be processed. Segmentation by watersheds is an extension of cluster fast segmentation that can to a great extent faithfully reproduce the particles without any requirements for image expansion. Segmentation by watersheds was first proposed by Lantuejoul (1978). The principle is to consider the successive stages in erosion of the original image as horizontal cross sections of a relief, from the highest elevation to the ground level. The watersheds will be the domains of attraction of rain falling over the region (Serra 1982). The various steps involved are as listed.

Step 1:
The first step in this technique is to create a distance map, where the brightness of each pixel is a measure of its distance from its boundary. Thus a gray-scale image is created from a binary image. The image is repeatedly eroded, and after each erosion, all remaining pixels have their brightness values incremented by one. At the end of Step 1, we have the desired distance map. The brightest points in the centers of features are the peaks of the mountains, and the valleys are the watersheds. The segmentation occurs along the watersheds.

$$\mathbf{X}_i = \mathbf{X} \ominus i\mathbf{B}, \quad for \quad i = 1 \cdots m \quad where \ `\{m : \mathbf{X}_m \neq 0\}. \tag{15}$$

Note that $\mathbf{X}_i$s for various i are different stages in the repeated erosion. The distance map is one image. It contains all ones at the start of Step 1. All the elements that disappear at the end of next erosion remain as one. The ones that remain become twos. This is continued until we get the final distance map which contains m, m-1, m-2,$\cdots$, 1.

Step 2:
This step is the same as Step 2 of Cluster fast segmentation. The ultimate eroded sets are obtained using the same principle in cluster fast segmentation. $\mathbf{Y}_i$s are the ultimate eroded sets.

Step 3: The various stages are as listed.

$$\begin{aligned} do \quad until \quad m &= 0 \\ \mathbf{Y}_m &= \mathbf{Y}_m \cup \mathbf{Y}_m \\ \mathbf{Y}_m &= \mathbf{Y}_m \odot \{\mathbf{T}^i\}; \mathbf{X}_m \\ m &= m - 1 \\ end \quad do. \end{aligned} \tag{16}$$

Starting from the final stage, the ultimate eroded sets are conditionally thickened with respect to the corresponding eroded set. Thus $\mathbf{Y}_m$ will be conditionally thickened with respect to $\mathbf{X}_m$. The thickening process is regulated such that it prevents any of the particles from reconnecting. This is made possible by using $\mathbf{T}^i$, which consists of twelve structuring elements (Russ 1990) as given in Figure 6. The twelve structuring elements are obtained by rotating each one of the three structuring elements in Figure 6 by ninety degrees four

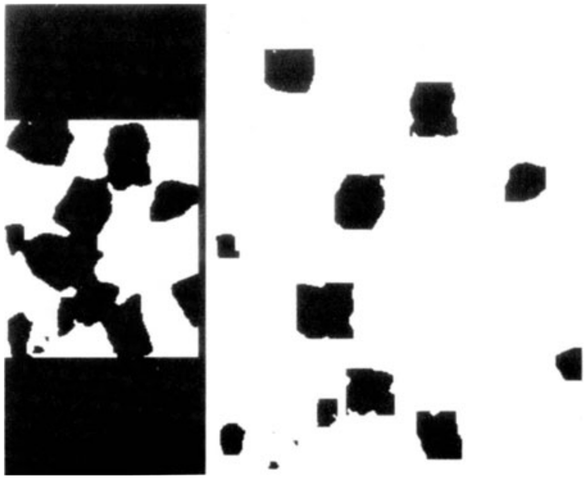

Figure 5. Result of applying Method 2.

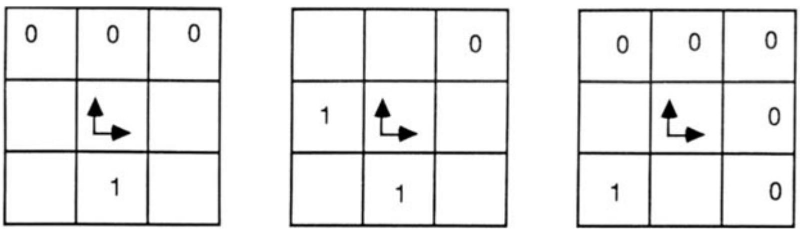

Figure 6. Structuring element used in watershed segmentation.

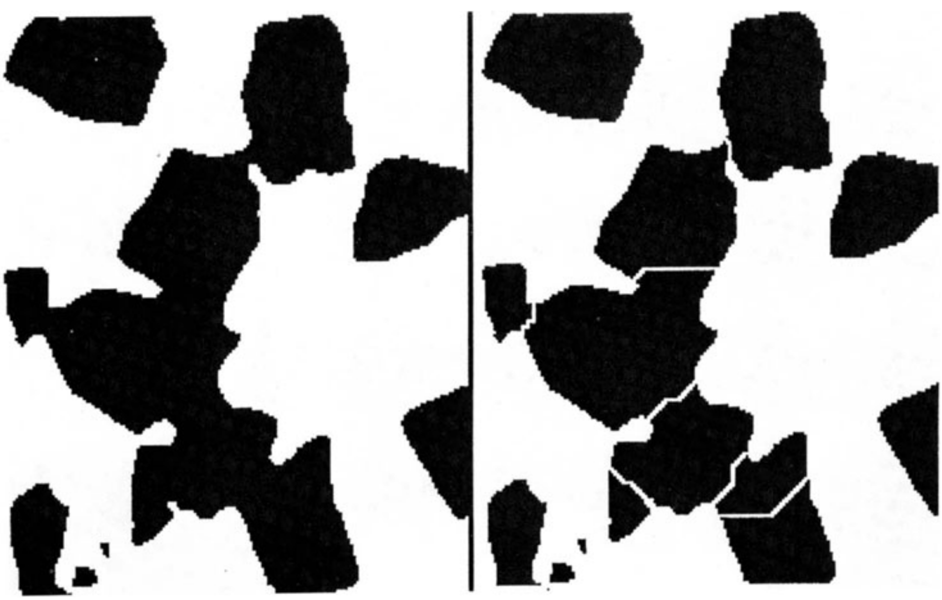

Figure 7. Result of watershed segmentation.

times. A 1 is placed at the origin only if the pixels marked 0 and the pixels marked 1 exist in the same format as the structuring element. Ultimate eroded sets from the corresponding stage are added on at each stage and the growth is limited to those points contained in the corresponding eroded stage. It is to facilitate this that the distance map was created. The corresponding eroded stage can be kept track using the brightness values in the distance map.

Figure 7b gives the result of watershed segmentation. It has done a great job in breaking the connectivity among the particles. There are cases when a particle has eaten into another particle. But there is no doubt that watershed segmentation outperforms all previous techniques discussed in this paper

CONCLUSION

Three techniques that can break the connectivity among the silicon carbide particles in aluminum metal matrix composites have been discussed. These techniques are fairly robust and can be used for other images to tackle similar problems. The performance improves in the order in which they were presented. The computational complexity also increases in the same order. Watershed segmentation is lot more time consuming than the three methods. But there are faster algorithms that have been mentioned recently in the literature. One case where Method 2 might do a better job than watershed segmentation is when the particles are greatly overlapped. In such a case image expansion could facilitate better reproduction of the particles.

ACKNOWLEDGEMENT

This work was supported by the Center for NDE at Iowa State University and was performed at the Ames Laboratory. Ames Laboratory is operated for the U.S. Department of Energy by Iowa State University under Contract No.W-7405-ENG-82.

REFERENCES

1. A. Rosenfeld, ''Connectivity in Digital Picture'', Journal of the Association for Computing Machinery, vol.17, pp. 146-160, Jan. 1970.
2. F. Meyer, ''Iterative Image Transformations on an Automatic Screening of Cervical Smears '', Journ. Histochem. Cytochem., vol.27, pp. 128-135, 1979.
3. J. Serra, Image Analysis and Mathematical Morphology, (Academic Press, London, 1982).
4. G. Matheron, Random Sets and Integral Geometry, (Wiley, New York, 1965).
5. L. Calabi, ''A Study of the Skeleton of Plane Figures'', Parke Mathematical Labs, Carlisle, MA, Rep. SR2-60429, June 1985.
6. C. Lantuejoul, ''Skeletonization in Quantitative metallography'', Issues of Digital Image Processing, R. M. Haralick and J. C. Simon, eds., Groningen, The Netherlands: Sijthoff and Noordhoff, 1980.
7. P. A. Maragos and R. W. Schafer, ''Morphological Skeleton Representation and Coding of Binary Images'', IEEE Trans. on ASSP, vol.ASSP-34, pp. 1228-1244, Oct. 1986.